Using city-wide mobile noise assessments to estimate bicycle trip annual exposure to Black Carbon

Luc Dekoninck[a)]
Dick Botteldooren[b)]
Information Technology, Acoustics Group, Ghent University
St-Pietersnieuwstraat 41, 9000 Ghent, Belgium[a,b]

Luc Int Panis[c,d)]
Flemish Institute for Technological Research (VITO), Boeretang 200, 2400 Mol, Belgium[c]
Transportation Research Institute (IMOB), Hasselt University, Wetenschapspark 5 bus 6, 3590 Diepenbeek, Belgium[d]

ABSTRACT

Several studies have shown that a significant amount of daily air pollution exposure, in particular Black Carbon (BC), is inhaled during bicycle trips. Previously, the instantaneous BC exposure of cyclists was modeled as the sum of a background concentration and a local traffic related component based on a local assessment of traffic noise. We present a fast and low cost methodology to achieve a city-wide assessment of yearly average BC exposure of cyclists along their trips, based on a city-wide mobile noise sensing campaign.

The methodology requires participatory sensing measurements of noise, partially combined with BC and/or other air pollutants sensitive to local traffic variations. The combined measurements cover the spatial and meteorological variability and provide the data for an instantaneous exposure model. The mobile noise-only measurements map the full city; and yearly meteorology statistics are used to extrapolate the instantaneous exposure model to a yearly average map of in-traffic air pollution exposure. Less than four passages at each segment along the network with mobile noise equipment are necessary to reach a standard error of 500 ng/m³ for the yearly average BC exposure.

A strong seasonal effect due to the BC background concentration is detected. The background contributes only 25% to the total trip exposure during spring and summer. During winter the background component increases to 50-60%. Engine related traffic noise along the bicyclist's route is a valid indicator of the BC exposure along the route, independent of the seasonal background. Low exposure route selection results in an exposure reduction of 35% in winter and 60 % in summer, sensitive to the weather conditions, specific trip attributes and the available alternatives.

The methodology is relevant for further research into the local effects of air pollution on health. Mobile noise mapping adds local traffic data including traffic dynamics into the air pollution exposure assessments. Local policy makers and urban planners can use the results to support the implementation of low exposure infrastructure, create awareness through route planners and achieve behavioral changes toward active travel modes.

Highlights

- Mobile noise level to within 2 dB is sufficient to estimate annual BC exposure of cyclists
- Mapping mobile noise provides city-wide yearly averaged in-traffic air pollution exposure
- A low-cost methodology for city-wide evaluation of noise and air pollution is presented
- Cyclists can reduce exposure by 35-60% through selecting low exposure routes

[a)] email: luc.dekoninck@intec.ugent.be (corresponding author, tel +32 9 264 99 95)
[b)] email: dick.botteldooren@intec.ugent.be
[c)] email: luc.intpanis@vito.be; luc.intpanis@uhasselt.be

1. Introduction

Exposure to particulate matter is currently regulated in PM standards that only distinguish between the size of the particles but not between the composition and thus origin of the particulate matter. The soot fraction or Black Carbon (BC) is a fraction of the PM directly related to combustion processes. Recent evidence, summarized by the World Health Organization (WHO), documents the relevance of BC for evaluating traffic related health effects (WHO Europe, 2012). BC is more sensitive to traffic emissions and is able to detect local exposure differences not available in the PM_{10} evaluations. The first epidemiological results based on BC exposure detect health effects up to ten times stronger compared to the similar evaluations based on PM_{10} (Janssen et al. 2011).

Large personal exposure measurement campaigns prove the relevance of the in-traffic exposure contribution to daily personal exposure (Dons et al., 2011, 2012). Technology for mobile air pollution measurements is however scarce and expensive. The high variability of the in-traffic exposure is partially due to the strong influence of meteorology on the exposure, swamping the variability due to the local traffic densities and dynamics (Dons et al., 2013). In previous work of the authors, an instantaneous spatiotemporal model based on mobile noise measurements for cyclists was proposed (Dekoninck et al., 2013). It was shown that noise measurements are a good proxy for local traffic intensity and local traffic dynamics. The instantaneous spatiotemporal model splits the BC exposure of a cyclist into a background component and a component of local origin. In the Flemish region, only one continuous monitoring station was available at the time of the measurement campaign that can act as a background concentration (Antwerpen-Linkeroever – 40AL01). After adjusting for the background contribution the local variation in the traffic density and traffic dynamics successfully predicts the BC exposure of the cyclists using four parameters: the low frequency noise (L_{OLF}) related to the traffic volume and engine throttle, the difference between high and low frequencies (L_{HFmLF}) relating to the traffic speed, the instantaneous wind speed and the street canyon index (StCan). Wind speed and street canyon features affect the dispersion of BC. The background adjusted model significantly reduced the temperature dependency of the bicyclist exposure. All temperature dependency, regardless of the origin (other BC sources, meteorology or vehicle fleet related aspects) is resolved in the background contribution. In other work, the instantaneous model approach was validated in completely different traffic

73 conditions (Bangalore, India). The quality of the background adjustment was related to the properties of the

74 background measurement location (Dekoninck et al, 2015). Meteorological conditions thus enter this model

75 directly through the wind speed and indirectly via temperature and wind speed in the background BC

76 concentration. Wind direction was not included in the model. The strongest component in the local traffic

77 related exposure is the traffic within meters from the cyclists, resulting in correlation of 0.86 with only four

78 parameters. Wind direction is not relevant at such small distances to the source. The noise measurements

79 quantify the local traffic and traffic dynamics. The strengths of the method are based on the possibility to

80 quantify the local traffic properties and by adding missing traffic data at low density traffic roads.

81   For many applications however, there is a strong interest in annual average rather than instantaneous

82 levels of exposure. The internal validation of the instantaneous model -predicting 25% of the trips using

83 models fit on the other 75% of the trips- resulted on average in a correlation of the trip averaged BC exposure

84 of 0.77 (Dekoninck et al., 2013). The intrinsic quality of the instantaneous model to predict a single trip under

85 any meteorological conditions or trajectory is strong and enables the simulation of yearly average exposure

86 during bicycle trips without further validation. One of the remaining questions is whether subtracting a

87 measured background concentration results in a valid local contribution that can actually be interpreted as

88 the contribution of the local traffic (BC_{loc}). If this is the case, the model should result in BC_{loc} approaching zero

89 with low traffic intensity. As an alternative, the behavior of the strongest component in the spatiotemporal

90 model, L_{OLF} is proposed as a good indicator of the background adjustment since this component is directly

91 related to the presence of traffic. When the spatiotemporal model reveals a linear relationship between L_{OLF}

92 and $\log(BC_{loc})$, the background adjusted exposure will by consequence only include local traffic related

93 exposure. For low L_{OLF}, the local contribution in the instantaneous model dwindles to values close to the

94 detection limit of the BC measurement equipment. Therefore the background location and the applied

95 background correction are valid.

96   In each mobile measurement campaign only a limited number of potentially occurring situations is

97 sampled. Bias is introduced into the measurements due to the combination of route choice, instantaneous

98 meteorological conditions and instantaneous background exposure, each of them subject to unintended

99 selection bias. It is therefore impossible to perform a measurement campaign covering all combinations of the

100 exposure variables with unbiased exposure as the result. This paper will therefore introduce a methodology

to convert a map of biased mobile measurements into a yearly average unbiased BC exposure map building upon the available instantaneous model (Dekoninck et al., 2013). This will be achieved in two phases. First the instantaneous exposure will be extrapolated to a yearly average by applying the spatiotemporal model for all meteorological situations to all available mobile noise measurements. In the second phase the instantaneous noise exposure is replaced by the average noise exposure at that location. In this way all dependence on meteorology can be removed, and the typical traffic situation at each location along the network is characterized using mobile noise measurements from a small but sufficient number of passages. This results in a spatial model, only based on local traffic related features (derived from noise) and a street canyon index (a parameter describing the accumulation of BC in narrow streets).

Several research questions will be addressed: how can a mobile noise measurement campaign be used to predict the annual average BC exposure for cyclists and how many noise measurement trips are necessary to reliably estimate the local traffic contribution. In addition, the effect of seasonal meteorological changes on the local traffic related BC exposure and on the total exposure will be illustrated. The potential exposure reduction by choosing low exposure routes is quantified.

2. Methodology and data processing

2.1 Methodology

The instantaneous model is based on 209 rush hour commuting trips by bicycle from the villages to the west of Ghent (Belgium) into the city center. More than 75 km of distinct roads were sampled at least 3 times. The BC measurements are performed with the micro-aethalometer AE51 (Aethlabs.com, San Francisco). The details are available in Dekoninck et al., 2013 and the supplementary data. The instantaneous log-transformed model will be referred to as $BC_{loc,temporal}$ in this paper. The subscript 'temporal' is added to avoid confusion with the spatial yearly average models that will be developed in this work. Thus, to obtain a meteorology averaged BC exposure of cyclists, only wind speed and background concentration have to be accounted for. To implement a correction towards yearly representative meteorological conditions, the meteorological conditions are categorized according to the meteorological dependencies in $BC_{loc,temporal}$: wind speed and background concentration. A joint distribution over these two variables should be used because

127 background BC concentration itself strongly depends on wind speed. The meteorological classes are
128 presented in Section 2.2.

129 To obtain a yearly averaged value, the $BC_{loc,temporal}$ model is applied for a sufficiently large number of
130 bicycle commuting trips passing through each evaluation point along the road network for each combined
131 meteorological - background concentration class observed during a year. This means that the instantaneous
132 wind speed and background concentration of that specific trip are replaced in the model by the wind speed
133 and background concentration of the evaluated meteorological class. For each spatial evaluation point, the
134 resulting dataset contains a BC estimate for each noise-measuring trip and each meteo/background class,
135 Met_{cl}. A weighted average is applied according to the frequency of occurrence during a year of Met_{cl}, merging
136 the results spatially for all trips passing by at a specific location.

137 In mathematical form, the procedure is summarized as follows. The local contribution to the measured BC
138 concentration $BC_{loc,meas,i,j}$ for a location i and during a trip j, is written as:

$$BC_{loc,meas,i,j} = BC_{tot,meas,i,j} - BC_{bg,j} \qquad (1)$$

140 Using the previously derived model, this contribution is approximated using Generalized Additive Models
141 (GAM) (Wood, 2006). Several authors in air pollution research have applied this technique successfully
142 (Dominici et al., 2002, Pearce et al., 2011, Li et al., 2013). The modeled BC concentration is obtained for each
143 location i during trip j as:

$$BC_{loc,temporal,i,j} = \exp(gamBC_{loc,temporal}(L_{OLF,i,j}, L_{HFmLF,i,j}, StCan_i, WS_j)) \qquad (2a)$$

$$BC_{tot,temporal,i,j} = \exp(gamBC_{loc,temporal}(L_{OLF,i,j}, L_{HFmLF,i,j}, StCan_i, WS_j)) + BC_{bg,j} \qquad (2b)$$

146 Note that all spatiotemporal dependence of the GAM model is implicitly included via the model covariates and
147 that the background contribution is assumed location independent. Applying the wind speed and BC
148 background concentration for all meteorological conditions Met_{cl} on each trip j:

$$BC_{loc,year,i,j} = \frac{1}{\sum_{Metcl} w_{Metcl}} \sum_{Metcl} w_{Metcl}(gamBC_{loc,temporal,i,j}) \qquad (3)$$

$$BC_{tot,year,i,j} = \frac{1}{\sum_{Metcl} w_{Metcl}} \sum_{Metcl} w_{Metcl}(gamBC_{tot,temporal,i,j}) \qquad (4)$$

151 Note that this result still has a weak dependence on trip number, and thus time, via the measured sound

152 parameters and via the chosen route at that specific time. By aggregating all measurement trips to a spatial

153 point p_i along the network, the spatial distribution is obtained:

$$BC_{loc,year,i} = \frac{1}{n}\sum_j BC_{loc,year,i,j} \tag{5}$$

154

$$BC_{tot,year,i} = \frac{1}{n}\sum_j BC_{tot,year,i,j} \tag{6}$$

155

156 Where for each spatial point p_i the collection of trips j passing point p_i contribute to the yearly average. In the

157 last phase, the instantaneous noise levels are replaced by the average noise levels at each location p_i. (eq. 7

158 and 8). All meteorological variability is included in the input data (eq. 5 and 6) and no instantaneous

159 meteorological covariates are necessary in the yearly meteorology based GAM models (eq. 9 and 10):

$$L_{OLF,i,map} = \frac{1}{n}\sum_j L_{OLF,i,j} \tag{7}$$

160

$$L_{HFmLF,i,map} = \frac{1}{n}\sum_j L_{HFmLF,i,j} \tag{8}$$

161

$$gamBC_{loc,year} \equiv \log(BC_{loc,year,i}) = gam\ (L_{OLF,i,map}, L_{HFmLF,i,map}, StCan_i) \tag{9}$$

162

$$gamBC_{tot,year} \equiv \log(BC_{tot,year,i}) = gam\ (L_{OLF,i,map}, L_{HFmLF,i,map}, StCan_i) \tag{10}$$

163

164 This results in a function that converts the average mobile noise measurement map to an average BC map,

165 independently of the trip sampling paths. In Figure 1, the spatial variability of the two noise covariates

166 ($L_{OLF,i,map}$ and $L_{HFmLF,i,map}$) and the street canyon index $StCan_i$ are illustrated, as well as the background

167 adjusted local component of the BC measurements ($BC_{loc,meas,i,map}$) spatially averaged in a similar way as the

168 noise covariates (eq. 7 and 8). Local BC contributions are highly variable and are affected by local traffic
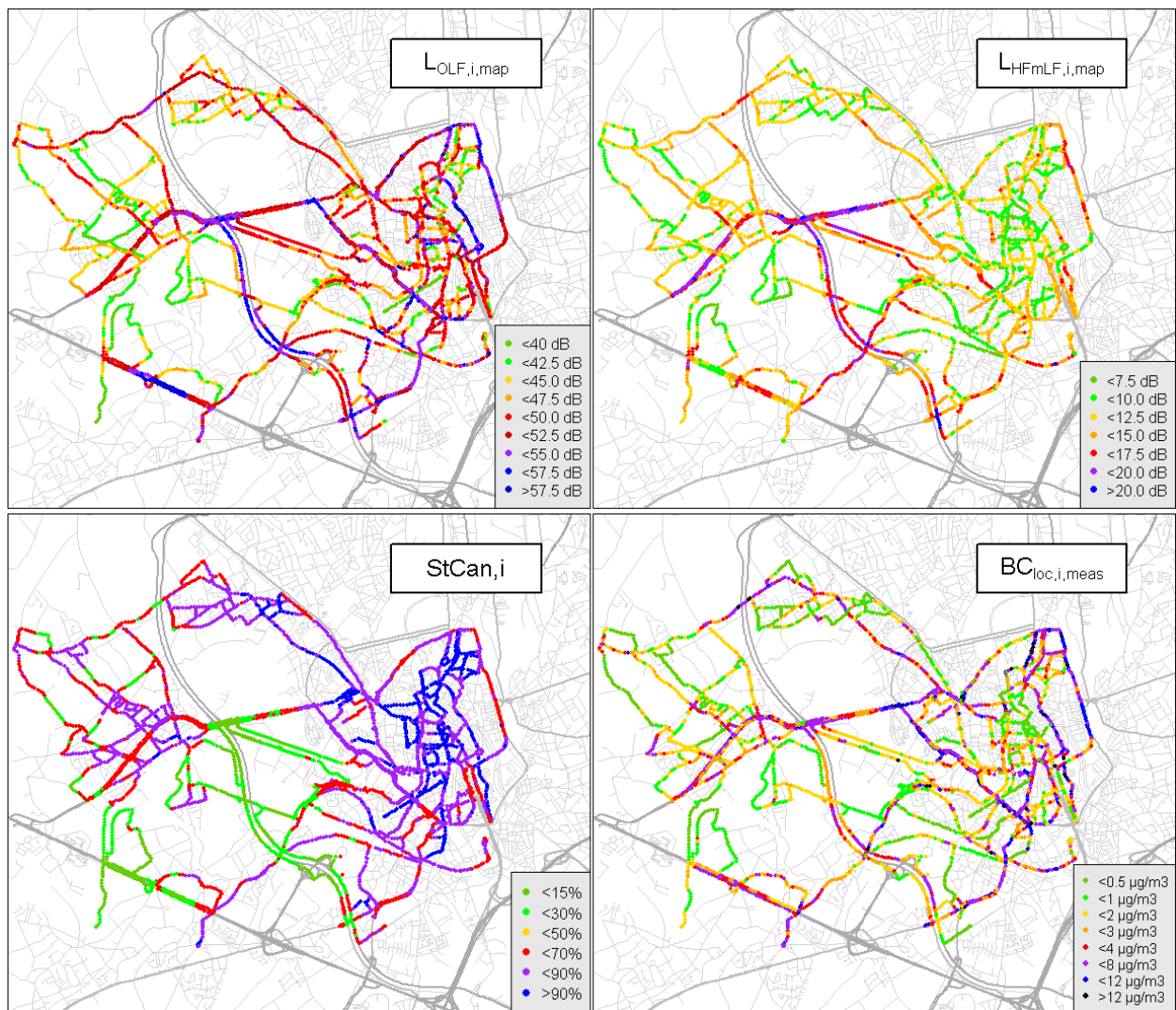
169 variability.

170

171

Figure 1: Three maps showing the spatial covariates ($L_{OLF,i,map}$, $L_{HFmLF,i,map}$ and $StCan_i$). The fourth map shows the average local contribution to the BC exposure measurements: $BC_{loc,meas,i,map}$.

2.2 Meteorology classes

The combined mobile noise and BC measurement campaign stretched from November 2010 till November 2011. The yearly averaged exposure was calculated for the calendar year 2011. A full year of hourly meteorological data for 2011 was retrieved from the national meteorological institute of Belgium (KMI). The measuring site is located in Melle, less than 10 km south of the city center of Ghent. BC background data covering the full year 2011 was made available by the environmental institute of Flanders (VMM) for the nearest station at Antwerpen-Linkeroever (40AL01). The same data were used for the background adjustment in the spatiotemporal model. Further information is available at http://www.irceline.be.

183   Only the meteorological conditions during the rush hour (7:00-10:00h and 16:00-19:00h) were included

184   in the statistics, since the model is only based on rush hour measurements. For the year 2011 this resulted in

185   160 distinct meteorological / background concentration classes (referred to as Met_{cl}), each class occurring in

186   the year 2011 with a weight $wMet_{cl,2011}$. The wind speed classes ranged from 0 to 11 m/s and the BC

187   background concentrations from 0 to 16 µg/m³. The distribution of the wind speed classes, BC background

188   classes and the combined occurrences are presented in Figure 2. The size of the circles is proportional to the

189   occurrence $wMet_{cl,2011}$ of the meteorological situations. The sparse BC background values above 7 µg/m³ were

190   added to the 7 µg/m³ class for easy presentation in the plot only.
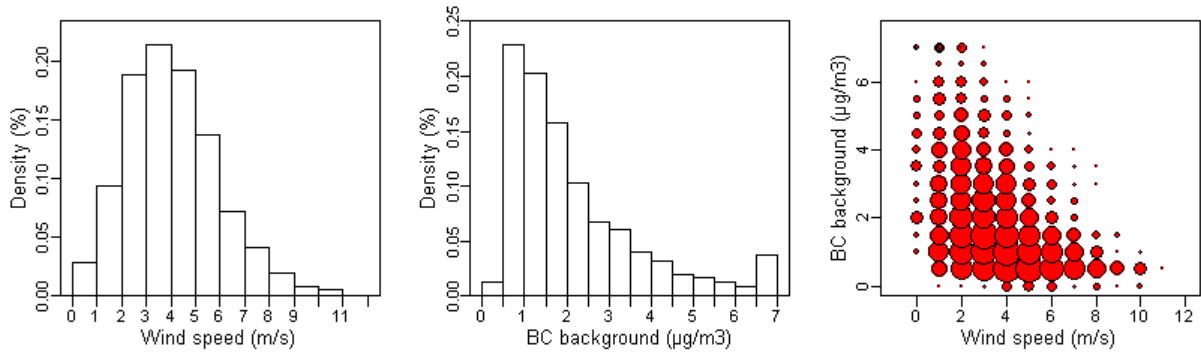

191
192   **Figure 2: Histograms of the wind speed (A), BC background exposure (B) and the combined**
193   **occurrence of wind speed and background exposure (based on hourly wind speed data in Melle and**
194   **30 minute BC data for station 40AL01 obtained respectively from VMM and KMI).**

195   # 3. Results

196   ## 3.1 A model for yearly averaged BC concentration

197   The data processing is based on data from Dekoninck et al, 2013, referred to as BDS. After applying Eq.(3)

198   and (4) on BDS the yearly meteorology adjusted BC exposure is available as $BC_{year,loc,i,j}$ and $BC_{year,tot,i,j}$ for each

199   location i and each trip j. The new datasets are representative for the yearly averaged meteorological

200   condition, removing the bias due to the not representative sample of meteorology of the trips that passed at

201   location i. A new GAM model containing only three parameters, L_{OLF}, StCan and L_{LFmHF}, can be extracted from

202   the new dataset, since the variability due to the wind speed is removed. The resulting models, $gamBC_{loc,year}$

203   and the $gamBC_{tot,year}$ are presented in Table 1. The GAM models are almost trivial and virtually perfect, since

204   they are based on the output of the $BC_{loc,temporal}$ GAM model. The only variability left in these GAM models is

205   the difference in the instantaneous noise evaluation covariates L_{OLF} and L_{HFmLF} for the trips contributing to the

206   location i.

Model	Intercept	$L_{OLF,i,map}$	$L_{HFmLF,i,map}$	StCan	Deviance explained	Number of points	AIC
			F-value		%	N	
gamBC$_{loc,year}$	8.11 (3.3 µg/m³)	37427	10272	18874	99.5	3827	-17064
gamBC$_{tot,year}$	8.60 (5.4 µg/m³)	17766	4395	8046	98.9	3827	-17980

207   **Table 1: Model results comparison, showing intercept, F-values, deviance explained and AIC.**

208   The gamBC$_{loc,year}$ model is the strongest model. The engine related noise covariate L_{OLF} is the strongest

209   component in both models. In Figure 3, the three spline plots including the residuals for L_{OLF}, L_{HFmLF} and StCan

210   are shown for gamBC$_{loc,year}$ and gamBC$_{tot,year}$. In gamBC$_{tot,year}$ the low traffic condition (small L_{OLF}) converges to

211   an lower limit, related to the yearly average BC background concentration. In the L_{OLF} covariate of

212   gamBC$_{loc,year}$ a very linear relation is found, even for low values. Traffic evaluation through noise assessment

213   has a perfect linear log-log relationship with the engine related noise after adjusting for the yearly

214   meteorology distribution. The speed related covariate L_{HFmLF} converges to a maximum. In situations with high

215   traffic speed the BC exposure does not increase any further for equal L_{OLF}. In the street canyon index a step-

216   like solution is visible. Below 0.5 the location is in rather open area, above 0.5, dispersion is significantly
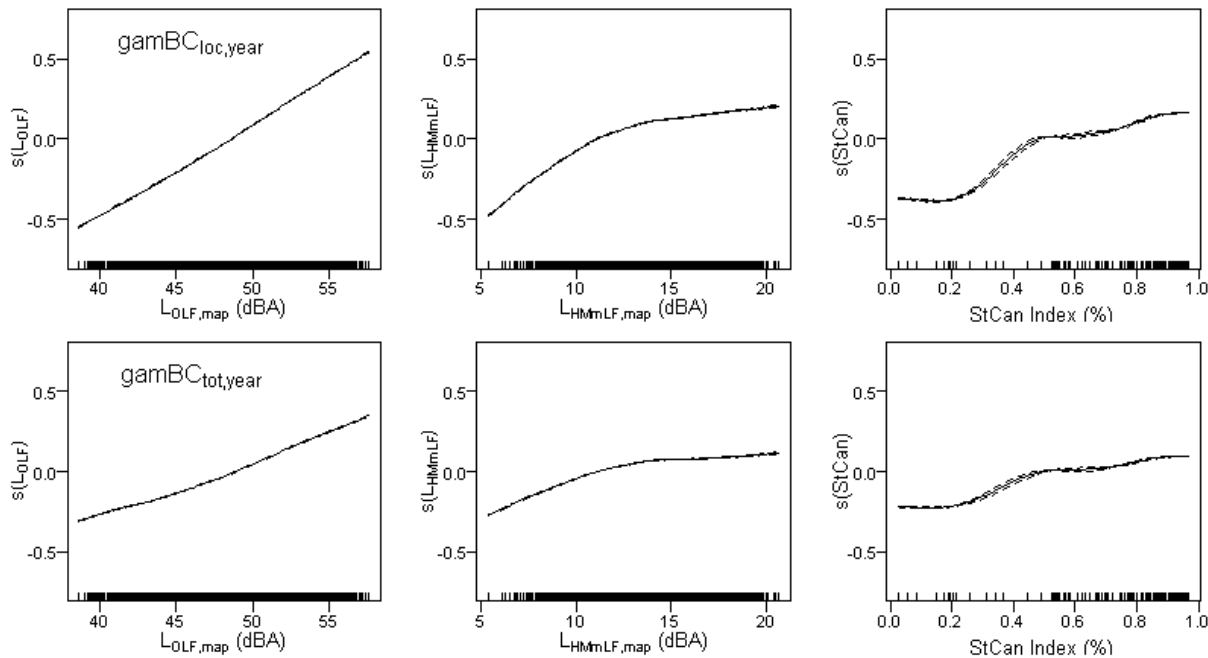
217   reduced.

218

Now we illustrate the effect of the different steps in modeling the yearly meteorology adjusted BC exposure using mobile noise data. A sequence of evaluations in Figure 4 illustrates the consecutive adjustments of the meteorology related effects on the bicyclist's exposure. The first evaluation (plot A) shows BC$_{tot,meas,j}$, the averaged measured BC exposure by trip (each dot is one trip) as a function of the strongest covariate L$_{OLF,meas,j}$, the averaged measured noise level L$_{OLF}$ along trip j. The correlation is low. After adjusting the exposure for the background contribution (BC$_{loc,meas,j}$) in plot B the correlation increases, but the wind speed is still an important variable in the personal exposure (see Dekoninck et al, 2013). The linear fit of the previous plot is repeated in the dashed line as a reference for each of the consecutive steps. In plot C the exposure is extrapolated to the yearly average meteorological conditions BC$_{loc,year,j}$ for each trip j. The correlation is enhanced up to 0.88 expressing the removal of the meteorology induced bias in the mobile measurement campaign. Several of the extremely high exposure trips are drastically reduced by applying the yearly average meteorology. The y-axis is adjusted to the new range. Plot D investigates the effect of replacing the actual noise measured along the trip by the average noise level for all passages at each location i passed by trip j, thus evaluating the trips according to the average mobile noise map for both noise covariates L$_{OLF,i,map}$ and L$_{HFmLF,i,map}$. Only a small change is detected for shifting from instantaneous noise level to the average over multiple passages, supporting the validity of replacing the instantaneous noise levels by the average noise levels. The correlation increases due to the removal of differences in the noise evaluation for trips passing at the same location i. Plot E replaces BC$_{loc,year,j}$ by BC$_{tot,year,j}$. The correlation is not affected since the difference is only related to the change in background exposure. The yearly average background adjustment is added.
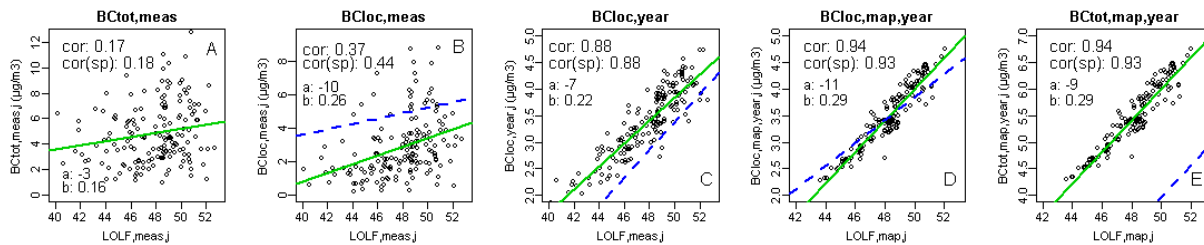

Figure 4: Visual representation of the sequential improvements of mobile measurements as a function of the trip average engine noise L$_{OLF}$: average measured BC$_{tot,meas,j}$ (A) along the trip and different exposure modeling steps: BC$_{loc,meas,j}$, BC$_{loc,year,j}$ BC$_{loc,year,map,j}$ and BC$_{tot,year,map,j}$.(B, C, D, E). Each

246 **plot includes a linear fit on the trip evaluation (green). The linear fit of the previous plot is repeated**
247 **in dashed blue on the next plot. Note the changes in the x and y-axis in the different steps.**

248 The spatial result of the gamBC$_{loc,year}$ and gamBC$_{tot,year}$ is presented in Figure 5. These maps are the yearly

249 meteorological adjusted version of BC$_{loc,meas,i}$ as presented in Figure 1. The maps are much smoother due to

250 the removal of meteo-related variability. They illustrate the sensitivity of the exposure to the local amount of

251 traffic, traffic dynamics and the distance of the bicyclist to the local traffic. The difference between BC$_{loc,year}$

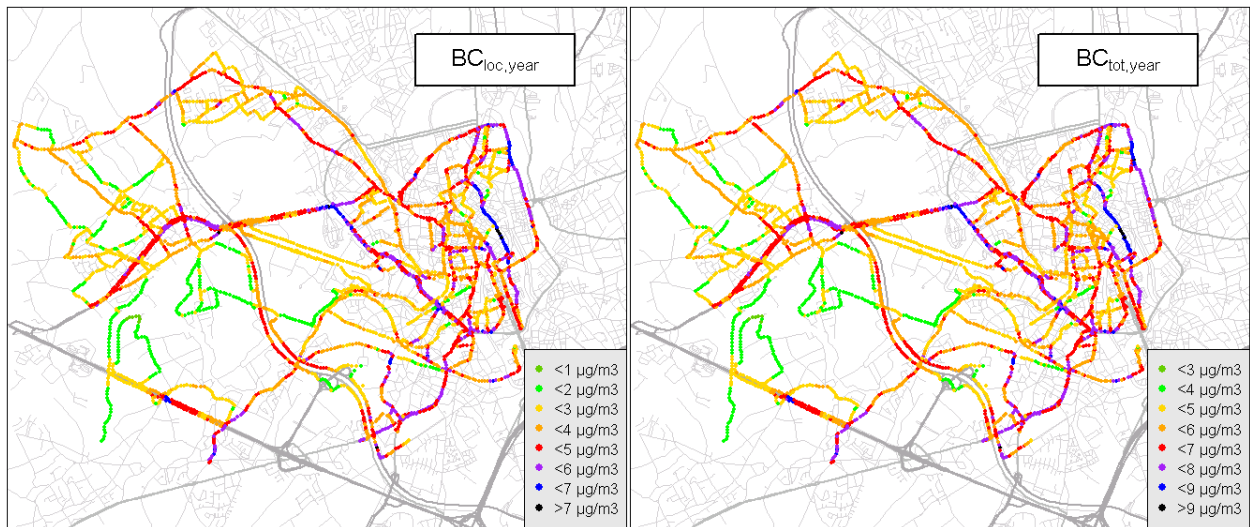252 and BC$_{tot,year}$ is a constant, the yearly averaged background adjustment.

253

254 **Figure 5: Visual representation of the yearly meteorology adjusted and noise mapped exposure**
255 **based BC exposure for cyclists: local component BC$_{loc,year}$ (left) and total exposure BC$_{tot,year}$ (right).**

256 ## 3.2 Number of noise measurements necessary for yearly
257 ## averaged BC prediction

258 Since bicyclist's BC exposure is highly sensitive to the meteorology, it is virtually impossible to achieve a

259 representative sample of measurements for all possible combinations of local traffic and meteorological

260 situations at a given location. Since the noise exposure at location i is not sensitive to the BC background

261 concentrations and much less sensitive to wind speed and wind direction compared to BC exposure, it is

262 expected that much less measurement repetition will be needed to quantify the local noise exposure at

263 location i compared to BC exposure. Hence, the measurement error on the yearly averaged BC exposure is

264 also expected to drop considerably with increasing number of trips. To confirm this expectation, the

265 measurement error (standard deviation over all trips divided by the square root of the number of trips that

266 contribute to the average) is calculated for each location *i* with two or more passages. Figure 6 shows box plot

267   statistics over all locations of this standard error for six parameters: $L_{OLF,i}$, $L_{HFmLF,i}$, $BC_{tot,meas,i}$, $BC_{loc,meas,i}$,

268   $BC_{tot,year,i}$ and $BC_{loc,year,i}$ as a function of the number of passages n. For $BC_{tot,meas,i}$ the standard error is not

269   significantly improving with increasing number of passages if the number of passages is below 10, illustrating

270   the high meteorology induced variability. That conclusion is also valid for $BC_{loc,meas,i}$, which is surprising since

271   a large portion of the meteorological effects is already removed from the dataset by adjusting for

272   instantaneous background exposure. For the yearly meteorology adjusted $BC_{tot,year,i}$ the standard error is

273   reduced dramatically. With as little as four passages, the Q3 of the standard error of $BC_{loc,,year,i}$ is smaller than

274   0.5. µg/m³. In this dataset 95% of all locations have a standard error for L_{OLF} below 2.0 dB and result in a

275   standard error below 0.5 µg/m³ for $BC_{loc,,year,i}$. For $BC_{tot,,year,i}$ four passages result in a Q3 smaller than 0.7.

276   µg/m³ and 90% of all locations in this dataset have a standard error for L_{OLF} below 2.0 dB and result in a

277   standard error below 0.75 µg/m³. Evaluating L_{OLF} within 2 dB accuracy is more than sufficient to characterize

278   the yearly averaged traffic related BC exposure.
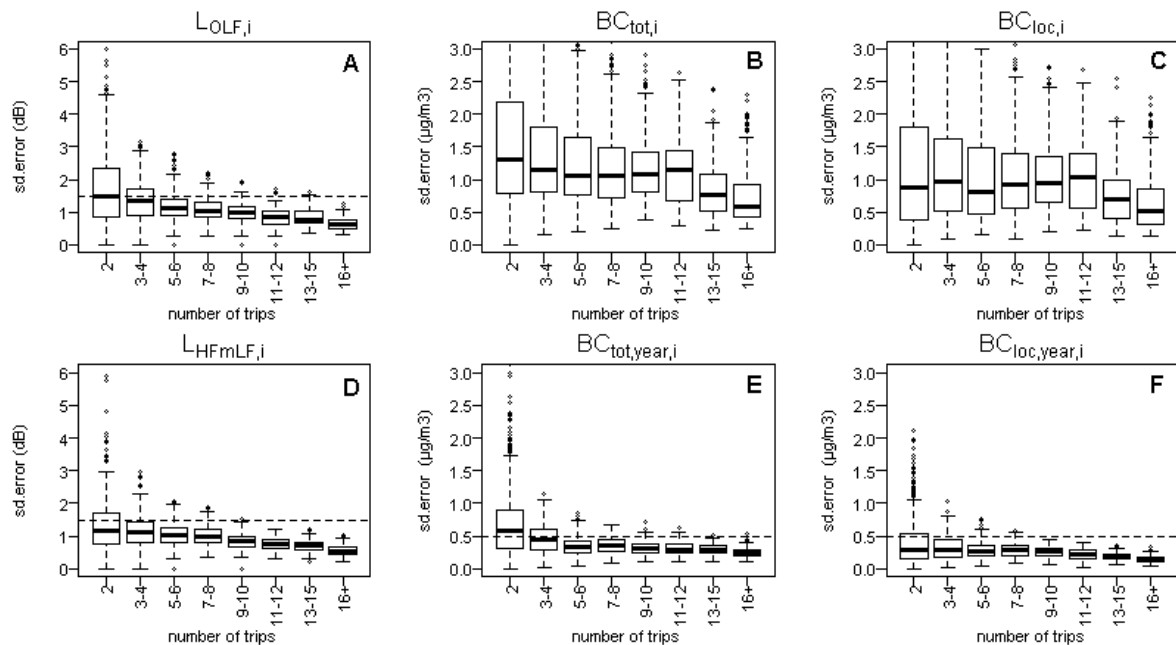
279

280   **Figure 6: Distributions of the standard error by number of passages at location i for $L_{OLF,i}$,**
281   **$BC_{tot,meas,i}$, $BC_{loc,meas,i}$, $L_{HFmLF,i}$, $BC_{tot,year,i}$ and $BC_{loc,year,i}$. Drop lines at 1.5 dB and 0.5 µg/m³ are added for**
282   **comparison.**

3.3 Monthly variation in BC exposure

In many countries the actual use of bicycles and the time spent outdoors depends on weather conditions and season. Hence, to correctly assess the yearly averaged exposure as well as to give advice to reduce personal exposure, one may need to account for the annual variation in meteorological conditions. In Figure 7A the evaluation over all trips is presented, while restricting the meteorological weighting to the occurrence of the meteorological conditions for that specific month: $BC_{loc,month,j}$ and $BC_{tot,month,j}$. The distributions indicate the range of the high to low exposure trips. The corresponding monthly meteorological statistics for the wind speed and background concentrations are shown in Figure 7B. Note the atypical conditions in December 2011 with high wind speeds and low background exposure. The variability of the wind speed by month does not show a strong seasonal pattern, and since this is the only meteorological covariate in the GAM model for $BC_{loc,month,j}$, $BC_{loc,month,j}$, does not show a seasonal pattern either. In this local situation, a yearly representative sample of wind speeds occurs each month. A strong seasonal effect on the $BC_{tot,year,j}$ is visible, expressing the strong seasonal effect of the background exposure. In Figure 7C the relative contribution of the background exposure to the local traffic component is shown. In summer, the local contribution is almost 75% of the total contribution, in winter it drops to 50%. For the larger part of the year, the local contribution is more than 60% of the total exposure.
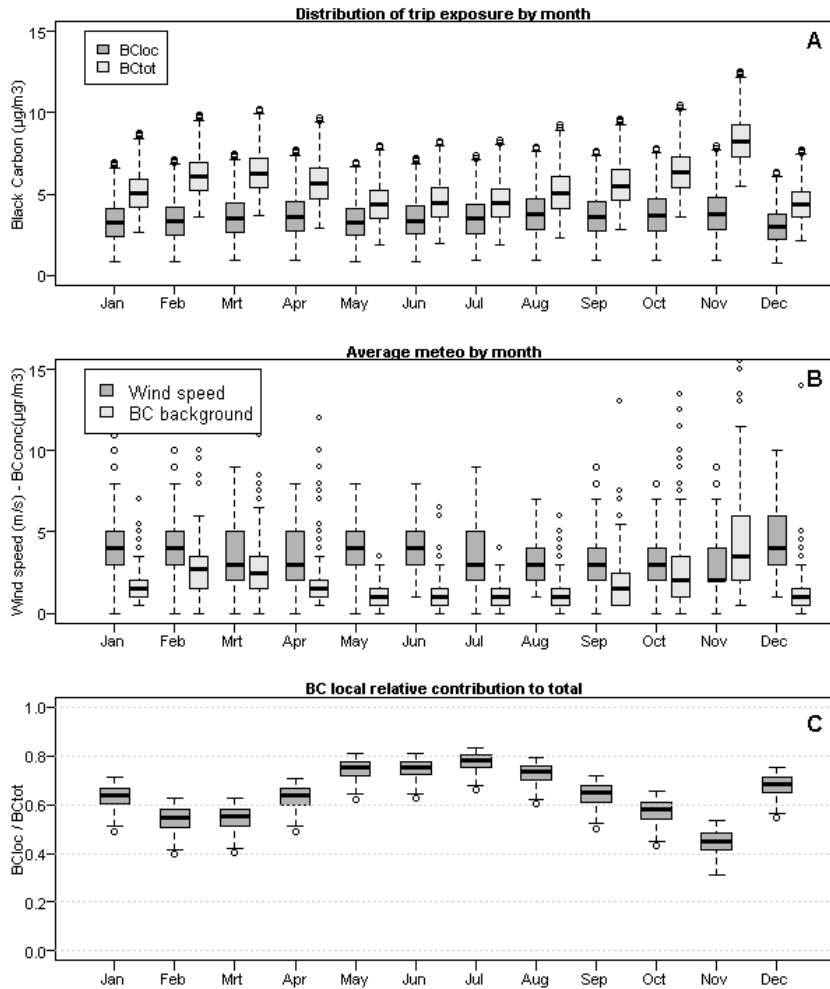
Figure 7: Monthly variation of the distribution of the local and total BC exposure by trip (A). Background BC and Wind speed show the effect of changing meteorological conditions over the year (B). Relative contribution of the local contribution to the total exposure (C).

3.4 City-wide mapping and low exposure routes

The proposed methodology for data collection uses mobile measurements on bicycle and consists of two simultaneous actions: during a limited set of trips BC and noise are measured jointly, preferably covering the full range of meteorological conditions and traffic conditions. These data are used to tune the coefficients in a local version of the $BC_{loc,temporal}$ model to the specific emission of the local vehicle fleet, meteorological conditions and background concentrations. The $BC_{loc,temporal}$ model is converted to the yearly meteorology adjusted GAM models as described in 2.1. An extensive mobile noise only measurement campaign can be performed to obtain spatial detail for a more extended area. In a numerical example: a city-wide participatory campaign with ten cheap noise measurement units, used by one-hundred participants for two weeks each can be completed in half a year. With a typical bicycle route of 10 km, each measuring their standard route and a

313   set of alternatives, will result in approximately 100 persons x 20 trips x 10 km or 20,000 km of mobile noise

314   data. If the participants' origins and destinations are well distributed over the investigated city and suburbs,

315   the majority of roads will be sampled adequately. The mobile noise measurements result in city-wide noise

316   maps $L_{OLF,i,map}$ and $L_{HFmLF,i,map}$. Mapping any bicycle trajectory to the mobile noise maps (within the extent of

317   the map) and applying the $BC_{loc,temporal}$ results in an instantaneous meteorological sensitive estimate of the BC

318   trip exposure. Applying the yearly or monthly meteorology adjusted models results in yearly or monthly

319   averaged BC exposure, according to the requirements of the application.

320   To estimate the potential exposure improvement of alternative route choice, we take a closer look at the

321   trips used for deriving the models presented in this article (Figure 4). Figures 4D and 4E show that trips

322   performed during rush hour result in differences in L_{OLF} of up to 10 dB with a matching reduction of over

323   50% in $BC_{loc,year}$ and 35% in $BC_{tot,year}$. A reference trip with an average $L_{OLF,map,trip}$ of 50 dB and an alternative

324   trip of 46 dB will result in a decrease of 1.3 µg/m3, a reduction of 33% for the local traffic component and

325   22% on the total exposure in a far from extreme trip change scenario. In interpreting the results one should

326   take into account that the travelled routes in this dataset were not optimized to detect the low exposure

327   routes. The travelled routes were by design always switching from high to low exposure road segments to

328   capture as much variability in traffic for similar meteorological conditions within a single trip. A systematic

329   choice for a low exposure route for commuting could easily result in a 35 to 60% reduction in personal

330   exposure depending on the season, but this also depends on the specific commute and the available

331   alternatives for that trip.

4. DISCUSSION

4.1 Predictive quality of the methodology

334   At first sight the GAM models deviance explained is extremely high. When considering the procedure and

335   the importance of the wind speed covariate in the spatiotemporal model, this is not surprising. All remaining

336   variability that is not explained by the spatiotemporal model is -by design- not available in the yearly

337   extrapolation. More important than the fact that the $gamBC_{loc,year}$ and $gamBC_{tot,year}$ models are virtually

338   perfect, is that all locations are included, even those that were sampled only once or twice, without affecting

339   the quality of the GAM model. It was expected that the dataset should be restricted to a minimum number of

340   passages to build a valid GAM model, but this was clearly not necessary. The quality of the model in the

341   locations with low sampling is also visible in Figures 6E and 6F. 75% of the points with only two passages

342   reach a yearly standard error below 500 ngr/m^3 for the gamBC$_{loc,year}$ and almost 50% reach this value for the

343   gamBC$_{tot,year}$ model. The procedure to adjust each individual trip to the yearly averaged meteorological

344   situation is effective. Dekoninck et al. (2012) concluded that an estimate of L$_{OLF}$ resulted in a standard error of

345   approximately 1.5 dB after ten samples at a specific location in similar traffic conditions. The results in this

346   paper show that a standard error of 1.5 dB does not have to be achieved to successfully apply this

347   methodology. A standard error of 2.0 dB is more than sufficient to result in a valid prediction of the yearly BC

348   exposure, which is achieved with four passages for a specific traffic condition. The data showed that it is

349   extremely difficult to achieve a valid averaged BC exposure by increasing the number of passages without

350   using the proposed modeling approach, as illustrated by the low reduction by number of trips in Figures 6B

351   and 6C. Noise measurements adequately quantify the local traffic situation and enable the disaggregation of

352   the variability in the BC measurements into local traffic related and meteorology related contributions. This is

353   valid for the instantaneous model and the yearly meteorology extrapolated model.

354   4.2 Comparison with other mobile measurements

355   A general review by Bigazzi and Figliozzi (2014) summarized 42 studies on the exposure of bicyclists.

356   Fourteen studies addressed BC or EC. The studies are combined and evaluated according to the reported

357   differences between high and low exposure road segments. The exposure on high exposure segments is 8

358   times higher than low exposure segments across the studies when excluding rural assessments. In the

359   measurements for the instantaneous model (reported in BC$_{loc,i,meas}$) the high exposure locations reach levels

360   up to 25 times the low exposure locations when including rural data and up to 10 times when excluding rural

361   data (see Figure 5). The evaluations in the instantaneous model are aggregated by 50 m segments. In the

362   review the data is aggregated by physical street segments. The measurements in the instantaneous model

363   also include high wind speed conditions and extreme background conditions, typically not sampled in bicycle

364   campaigns. These differences in the measurement setup (spatial detail and sampled meteorological

365   conditions) explain the larger detected ranges. Despite the differences in the measurement setup, the

366   measurement ranges are comparable with the results in the review.

4.3 Potential of background adjusted models

The additive modeling approach has the potential to be more than a mathematical method to disentangle the meteorological and background exposure effects from the local traffic contribution. Several authors investigated the particle size distribution in relation to the distance to the source (Karner et al., 2010, Boogaard et al., 2011, Strak et al., 2011, Kingham et al., 2013, Holder et al., 2014). All results show similar trends; closer to the source the size distributions show higher numbers of small particles. In health effects of air pollution exposure research, the importance of the particle size and particle count has been investigated by different authors (Strak et al., 2010, Seaton et al., 1995). Although the smallest particles may enter the body in different ways (e.g. through the olfactory nerve (Oberdorster, 2004)), specific health effects or different toxicity estimates (based on particle mass or on particle number and size distributions) have proven hard to detect (Osunsanya et al., 2001). The additive approach -splitting exposure in background particles (aged and larger) and local contribution (fresh and small)- can be a base for adjusting the exposure to particle size corrected exposures and to verify if high local contributions result in adverse health effects. Quantifying the particle size distribution adjustments for the local and background contribution is subject to further research. Similar measurement campaigns measuring UFP particle counts or particle size distributions can add significant value in this respect. A smaller measurement campaign has already shown that this technique is also valid for UFP (Dekoninck et al., 2015). UFP shows a steeper relation to L_{OLF} compared to BC and the additive approach is less sensitive to the background concentrations compared to BC.

4.4 Diurnal variability, vehicle fleet composition and policy support

The main limitation in the presented results is the restriction to rush hour exposure and traffic, the data limitation of the underlying instantaneous model. Since most policy measures are mainly focusing on commuting, the presented results are applicable in that context. The proven effectiveness of the noise sampling implies that mapping the traffic related exposure has the potential to be extended to capture the diurnal variability with only a small extension of the sampling strategy to include trips outside the rush hour and adding the hour of the day as a new dimension in the models. Only few passages on different types of routes for different times of the day could reveal the diurnal patterns of the BC exposure. Implementing this technique in other countries and/or continents requires recalibration of the instantaneous model. Vehicle fleet, vehicle fleet evolution, driver behavior, biking facilities, city characteristics, meteorological conditions

395   and air pollution background concentration all have their specific influence on the relationship between noise

396   and local traffic related air pollution. The sensitivity of the spatiotemporal model at different locations should

397   be evaluated for other dependencies (temperature, humidity etc.). Validating new implementations is crucial

398   and will not only illustrate the proposed methodology but will also detect effects of different vehicle fleets.

399   This must be seen as one of the most important applications of the combined methods (instantaneous

400   modeling and yearly meteorology adjusted maps). The instantaneous models will adjust and resolve the bias

401   between the different mobile measurement campaigns for meteorology, background concentrations, route

402   choice and traffic dynamics. The remaining difference can be attributed to the different fleet composition. In

403   Belgium more than 60% of the vehicles use diesel, a well-known source of BC. Large changes in the

404   relationship between noise and BC in other countries are probable and will be relevant for policy decisions in

405   Belgium. Consecutive calibration measurement campaigns are relevant to quantify the changes in the vehicle

406   fleet emission over time and require similar control over the sampling biases to reveal the vehicle fleet

407   related component in the evolution of the BC exposure. The effects of changes in the local and the background

408   exposure due to changes in the vehicle fleet emission or other BC sources are automatically included through

409   the background adjusted approach of the instantaneous model. This leads us to an important feature of the

410   mobile noise based traffic assessments. Noise emission of the vehicle fleet is much less sensitive to change

411   over time due to much less restrictive and less effective legislation for the noise emission of the vehicle fleet.

412   The traffic quantification is therefore valid for longer periods of time. Only reduced combined noise-BC

413   measurement campaigns are required to reassess the noise-BC relation. In response to local policy based

414   traffic changes, small dedicated 'noise-only' measurements can reassess the traffic densities and traffic

415   dynamics. The burden and costs of performing large air pollution measurement campaigns can be reduced

416   significantly while the results cover much larger areas.

417   From a scientific point of view, the improvement of personal exposure assessment for bicyclists to traffic

418   related air pollution is the most important goal of this methodological exercise. From the cyclist's point of

419   view, the awareness of their route choice on the related exposure is the most important aspect. Only if people

420   are aware of an issue, they can react and change their behavior accordingly. The main traffic related challenge

421   of the local governments is reducing car use within cities and promoting a shift to other modes of

422   transportation. A campaign similar to the proposed setup can inform the public on low exposure routes for

423 cyclists and the local government can use this information to improve the quality, availability and

424 dissemination of the alternative routes. Missing links in the biking network can be detected and benefits of

425 investing in these trajectories can be quantified and used in the dissemination process. Alternative routes and

426 improved bicycle infrastructure will also reduce the number of bicycle accidents (Reynolds et al., 2009,

427 Vandenbulcke et al., 2014, Molino et al., 2009).

4.5 Multidisciplinary aspects and LURs

429 The mobile noise mapping should not be only performed for air pollution assessments but can also be a

430 part of extended multidisciplinary evaluations of in-city traffic related livability. Strong synergies exist

431 between local air pollution exposure assessments and traffic noise related burdens. Local traffic assessment

432 along the roads near the dwellings improves noise annoyance and wellbeing evaluations of the inhabitants

433 (Botteldooren et al., 2010). Mobile noise measurements include more detail than calculated noise maps and

434 have the potential to add value to all environmental noise related evaluations. They also provide a proxy for

435 traffic on low-density roads where no external traffic data is available. An important application is the

436 improvement of the traffic related air pollution land-use regression models. The mobile noise map provides

437 traffic data for the LUR models on low density roads including local traffic dynamics. In the acoustic field, the

438 combination of mobile and fixed noise monitoring stations will enable dynamic noise maps (Can et al., 2011,

439 Can et al., 2014). City-wide mobile noise evaluation is therefore a strong tool to improve in-city livability in a

440 multidisciplinary approach.

5. CONCLUSIONS

442 We have successfully extended an instantaneous exposure model for bicyclists to a yearly meteorology

443 averaged exposure model. Strong seasonal effects were detected. Mapping the local variability of in-traffic

444 exposure to BC for cyclists based on mobile noise measurements can be achieved with a small number of

445 passages, since the noise exposure assessments are much less influenced by meteorological conditions and

446 are therefore more efficient compared to in-traffic air pollution assessments. Extending the presented models

447 to diurnal exposure models becomes feasible.

448 In low background conditions the background BC exposure accounts for less than 25% of the bicyclist's

449 exposure, whereas in high background exposure conditions the contribution is 40 to 60%. Low exposure

route choice can reduce the local traffic exposure with at least 35-60% depending on the available alternative trajectories and the season. Local governments can use mobile noise mapping to support investments in alternative networks for cyclists.

The results support the potential of the additive approach defining personal exposure as the sum of a background contribution and a local traffic contribution. Applying this technique enables international comparison of both the local traffic related particulate matter exposure and the background exposure levels. Applying the methodology on a city-wide scale will result in a detailed spatial and accurate yearly averaged exposure map. The influence of instantaneous meteorology on air pollution exposure can be quantified through a partial participatory sensing campaign measuring one or more traffic related air pollutants for the full range of meteorological conditions in parallel to the mobile noise measurement campaign mapping the full city. Extrapolation to yearly local and total exposure with or without seasonal adjustments is inherently available in the methodology. This low cost methodology quantifies the local traffic in an unprecedented spatial resolution and fits in a multidisciplinary approach of evaluating and improving personal exposure, livability, wellbeing and health in large urban and suburban context.

6. REFERENCES

Bigazzi, A. Y., & Figliozzi, M. A. (2014). Review of Urban Bicyclists' Intake and Uptake of Traffic-Related Air Pollution. Transport Reviews, 34(2), 221-245.

Boogaard H., Kos G.P.A., Weijers E.P., Janssen N.A.H., Fischer P.H., et al. 2011. Contrast in air pollution components between major streets and background locations: Particulate matter mass, black carbon, elemental composition, nitrogen oxide and ultrafine particle number. Atmospheric Environment, 45, 650-658.

Botteldooren D., Dekoninck L. & Gillis D. 2011. The Influence of Traffic Noise on Appreciation of the Living Quality of a Neighborhood. International Journal of Environmental Research and Public Health, 8, 777-798.

Can A., Dekoninck L. & Botteldooren D. 2014. Measurement network for urban noise assessment: Comparison of mobile measurements and spatial interpolation approaches. Applied Acoustics, 83, 32-39.

Can A., Van Renterghem T., Rademaker M., Dauwe S., Thomas P., et al. 2011. Sampling approaches to predict urban street noise levels using fixed and temporary microphones. Journal of Environmental Monitoring, 13, 2710-2719.

479   Dekoninck, L.; Botteldooren, D.; Int Panis, L., Guidelines for participatory noise sensing based on analysis of
480   high quality mobile noise measurements. Internoise 2012 (conference), 394-402

481   Dekoninck L., Botteldooren D. & Int Panis L. 2013. An instantaneous spatiotemporal model to predict a
482   bicyclist's Black Carbon exposure based on mobile noise measurements. Atmospheric Environment, 79,
483   623-631.

484   Dekoninck L., Botteldooren D., Panis L.I., Hankey S., Jain G., et al. 2015. Applicability of a noise-based model to
485   estimate in-traffic exposure to black carbon and particle number concentrations in different cultures.
486   *Environment International*, 74, 89-98.

487   Dominici F., McDermott A., Zeger S.L. & Samet J.M. 2002. On the use of generalized additive models in time-
488   series studies of air pollution and health. American Journal of Epidemiology, 156, 193-203.

489   Dons E., Panis L.I., Van Poppel M., Theunis J. & Wets G. 2012. Personal exposure to Black Carbon in transport
490   microenvironments. Atmospheric Environment, 55.

491   Holder A.L., Hagler G.S.W., Yelverton T.L.B. & Hays M.D. 2014. On-road black carbon instrument
492   intercomparison and aerosol characteristics by driving environment. Atmospheric Environment, 88,
493   183-191.

494   Janssen N.A.H., Hoek G., Simic-Lawson M., Fischer P., van Bree L., et al. 2011. Black Carbon as an Additional
495   Indicator of the Adverse Health Effects of Airborne Particles Compared with PM_{10} and $PM_{2.5}$.
496   Environmental Health Perspectives, 119, 1691-1699.

497   Karner A.A., Eisinger D.S. & Niemeier D.A. 2010. Near-Roadway Air Quality: Synthesizing the Findings from
498   Real-World Data. Environmental Science & Technology, 44, 5334-5344.

499   Li L.F., Wu J., Hudda N., Sioutas C., Fruin S.A., et al. 2013. Modeling the Concentrations of On-Road Air
500   Pollutants in Southern California. Environmental Science & Technology, 47, 9291-9299.

501   Molino J.A., Kennedy J.F., Johnson P.L., Beuse P.A., Emo A.K., et al. 2009. Pedestrian and Bicyclist Exposure to
502   Risk Methodology for Estimation in an Urban Environment. Transportation Research Record, 145-153.

503   Oberdorster G., Sharp Z., Atudorei V., Elder A., Gelein R., et al. 2004. Translocation of inhaled ultrafine
504   particles to the brain. Inhalation Toxicology, 16, 437-445.

505   Osunsanya T., Prescott G. & Seaton A. 2001. Acute respiratory effects of particles: mass or number?
506   Occupational and Environmental Medicine, 58, 154-159.

507   Pearce J.L., Beringer J., Nicholls N., Hyndman R.J. & Tapper N.J. 2011. Quantifying the influence of local
508   meteorology on air quality using generalized additive models. Atmospheric Environment, 45, 1328-
509   1336.

510   Reynolds C.C.O., Harris M.A., Teschke K., Cripton P.A. & Winters M. 2009. The impact of transportation
511   infrastructure on bicycling injuries and crashes: a review of the literature. Environmental Health, 8.

512   Seaton A., Macnee W., Donaldson K. & Godden D. 1995. PARTICULATE AIR-POLLUTION AND ACUTE HEALTH-
513   EFFECTS. *Lancet*, 345, 176-178.

514   Strak M., Boogaard H., Meliefste K., Oldenwening M., Zuurbier M., et al. 2010. Respiratory health effects of
515   ultrafine and fine particle exposure in cyclists. Occupational and Environmental Medicine, 67, 118-124.

516   Strak M., Steenhof M., Godri K.J., Gosens I., Mudway I.S., et al. 2011. Variation in characteristics of ambient
517   particulate matter at eight locations in the Netherlands - The RAPTES project. Atmospheric
518   Environment, 45, 4442-4453.
519   Vandenbulcke G., Thomas I. & Panis L.I. 2014. Predicting cycling accident risk in Brussels: A spatial case-
520   control approach. Accident Analysis and Prevention, 62, 341-357.
521   WHO Europe, 2012: Health effects of black carbon, ISBN: 978 92 890 0265 3.
522   Wood S.N. 2006. On confidence intervals for generalized additive models based on penalized regression
523   splines. Australian & New Zealand Journal of Statistics, 48.

524